




## Case Study

# Adjustment of glacier geometries to future equilibrium line altitudes in the Shigar River Basin of Karakoram Range, Pakistan

Siddique Ullah Baig<sup>1</sup>  · Fakhra Muneeb<sup>2</sup>

Received: 3 November 2020 / Accepted: 5 March 2021 / Published online: 20 March 2021

© The Author(s) 2021 

## Abstract

Pakistan's Karakoram region has a large variety of glacier types. Equilibrium line altitude (ELA) of alpine or valley glaciers represents mass balance. Field observations for estimation of ELA of the majority of Karakoram's glaciers are not available due to rugged glacier-covered terrains and lack of climatic data above 5000 masl. Therefore, we applied the hypsometrically controlled accumulation area ratio (AAR) and accumulation area balance ratio (AABR) methods for ELA estimation and glacier–climate reconstructions in the Shigar River Basin of the Karakoram region. Constrained by mountain topography, larger size and type of glaciers, several ranges of ELA are calculated and implemented for several ratios. Two parameters (ratio and interval) are provided to calculate AAR-ELAs between 0.4 and 0.8 with 0.05 interval and AABR-ELAs between 0.9 and 4.4 with 0.01 interval. By providing constant AAR (rather than constant glacier area), this approach adjusted glacier geometries (area) to future ELA variations. For constant AAR of 0.4–0.45, a 90-m ELA decrease from 5769 to 5679 m of Baltoro glacier adjusted its geometries by reducing ~5% area. The highest decrease of 140-m ELA of the same glacier is reported for constant AAR of 0.7–0.75, revealing a significant loss of 8% geometries. The projected geometry losses for all these glaciers are highly variable, with top-heavy glaciers (Biafo and Baltoro) projected to experience the major losses in glacier-ice area. It is concluded that the quality of ELAs is highly dependent on the reconstructed three-dimensional glacier surfaces.

**Keywords** Karakoram · Equilibrium line altitude · Mass balance · AAR · AABR

## 1 Introduction

Within Hindu Kush Himalaya (HKH), Karakoram Range has the highest share of the glaciated area with approximately 37% of the area under glaciation [4] with 10% being debris covered [20]. Pakistan's Karakoram region has a large variety of glacier types (e.g. avalanche nourished, snow and ice avalanches nourished, snow-fed and small-ice mass fed) [8, 9, 13, 19, 33, 34] and climatic conditions, but glacier characteristics are still only poorly known [16]. Particularly, estimation of equilibrium line altitude (ELA, the separating contour between a glacier's accumulation and ablation

area) becomes hard to accomplish because zero mass-balance (the net variation in glacier mass over a fixed year) observations of the majority of Karakoram's glaciers are not available [35]. The rugged glacier-covered terrains and severe climatic conditions in the Karakoram lead to scarcity in field observations. Historically, ELAs of two glaciers: Biafo [14] and Baltoro [24] of Shigar River Basin (SRB), were derived by using field data. Despite obtaining many years of snowline height values, Hewitt [13] expresses doubt pertaining to estimates and placement of glacier ELAs. Secondly, the ELA can hardly be detected as an unbroken line at the same altitude traversing the entire extent of the

✉ Siddique Ullah Baig, sbbaig@cuiatd.edu.pk; siddiquebaig@gmail.com; Fakhra Muneeb, fmuneeb.mses2018iese@student.nust.edu.pk | <sup>1</sup>High Mountain Research Center, Development Studies, COMSATS University Islamabad (Abbottabad Campus), Abbottabad 22044, Pakistan. <sup>2</sup>Department of Environmental Sciences, Institute of Environmental Sciences and Engineering, National University of Science and Technology (NUST), Islamabad 44000, Pakistan.



existing glacier, due to localized topographic and climatic disparities in ablation and accumulation [3, 15]. However, gaps in knowledge are decreasing substantially in recent years, thanks to increased use of satellite imagery and digital elevation models (e.g. to compile glacier inventories or derive ELAs) and availability of geographic information system (GIS)-based ELA estimation methods [7, 30, 41]. Altitude area ratio (AAR), the ratio of accumulation area to the total glacial area of the glacier (Meier, 1962), is used by many studies independently or in a combination of other methods. Lachniet and Seltzer [18] individually estimated hypsometry-based ELA by using both methods AAR and altitude area balance ratio (AABR) for high-elevation mountain glaciers in the Tamanca Range of Costa Rica and Taiwan. Stansell et al. [39] used the same method for nine palaeo-glaciers in the Venezuelan Andes. Only AAR method is applied to estimate ELA of Alaska and north-west Canada glaciers [22], Li and Li 2014), while three-year mean ELAs for 13 glaciers of Hunza River Basin are derived in a combination of other methods (Shrestha et al. 2017). Alternatively, snowlines, or steady limits on glaciers, are generally considered as reasonable estimates to ELAs and year-to-year AAR and to reflect mass-balance variations [11].

SRB (study area) (Fig. 1a) is one of the eight Upper Indus subbasins (i.e. Astor, Gilgit, Hunza, Shingo, Shigar, Shyok, Zaskar and Upper Indus). Out of the 21,192-km<sup>2</sup> snow and glacial-ice area in Upper Indus Basin, SRB has the highest glacial area followed by Hunza and Shyok [2]. The focus of this study is to estimate ELAs of SRB glaciers based on AAR and AABR methods as there is a lack of field data for ELA calibrations. Therefore, glacier ELA reconstructions are based on implicit and optimal AAR and AABR values. These methods have been applied for reconstruction of glacier–climate geometries in the mountain ranges worldwide (e.g. [5, 17, 29, 31]). However, these methods take glacier geometry derived from the topography [30]. Additionally, AABR takes mass-balance gradient into account as well. Out of the total 439 glaciers [38] of the study area, we selected four glaciers (Baltoro, Biafo, Panmah and Chogo Lungma) (Fig. 1b) due to their location, larger sizes and type. Furthermore, the studied glaciers cover 70.25% or 1534-km<sup>2</sup> (approximately two-thirds) of glacial area of the study area. Secondly, these glaciers are nourished by medium- or small-sized glaciers or tributaries which contribute melt water significantly to Indus River rise due to their shorter response times. A GIS-based automatic tool developed by Pellitero et al. [30] has been employed to estimate glacier ELAs for a series of AAR (0.4–0.8) and AABR (0.9–4.4) values. We used the AAR value of 0.6 and AABR value of 2.24 for their respective zero mass-balance estimation due to their high-altitude mountain topography. Iteratively, ELAs are estimated followed by balance-ratio

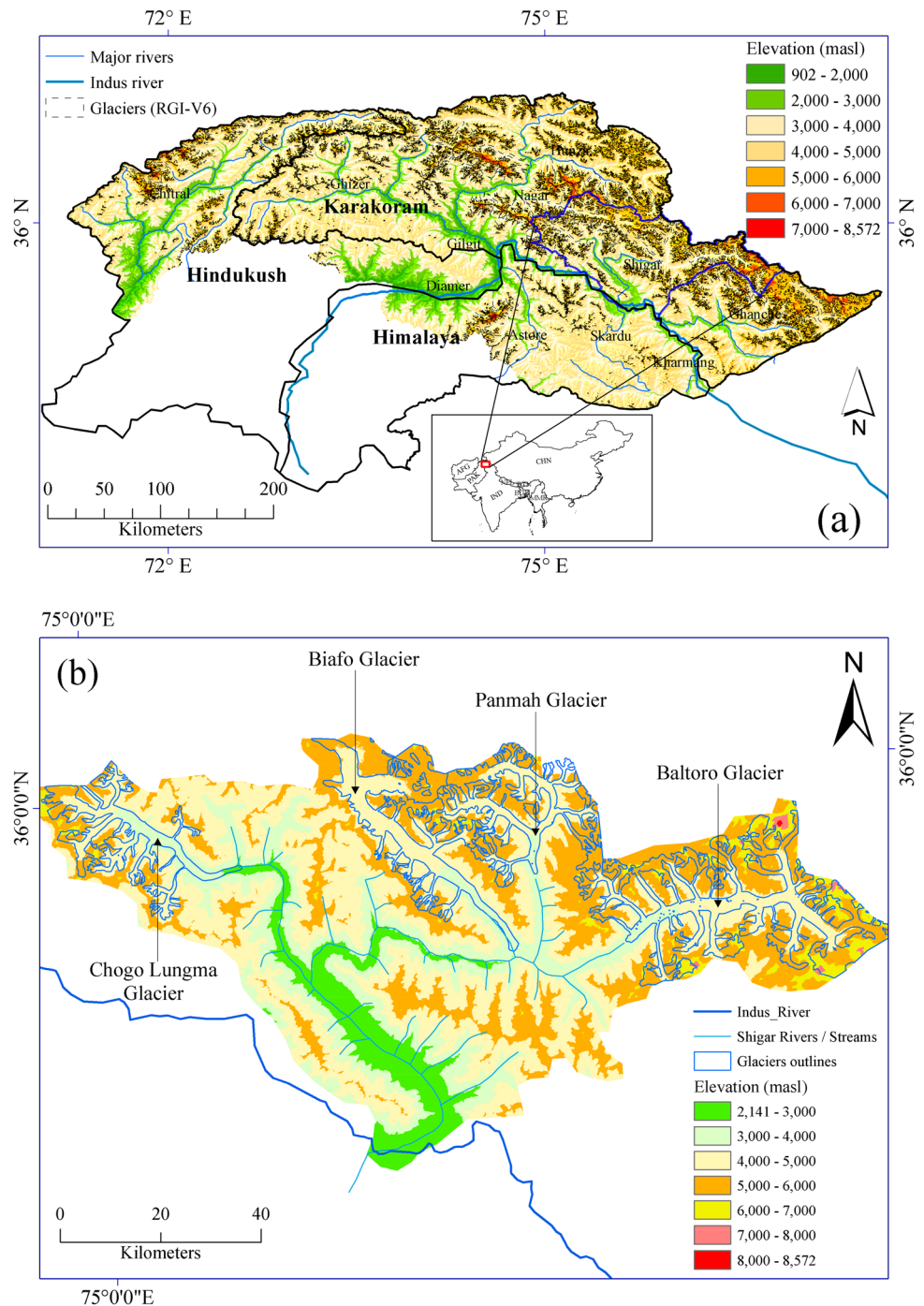
adjustments. Altitudinal land area covered by the glacier away from the ELA (either negative or positive) is assumed to have a greater influence to overall mass balance than glacial area that lies nearby to the ELA. The proportions of glacier breadth to ablation at snout are considered to be good indicators of response time of glacier volume [36]. Therefore, the likely mass losses under different ratios are determined above and below the ELAs. Furthermore, an attempt is made to create a relationship between vertical and horizontal climatic regimes of glaciated and non-glaciated landscapes of SRB.

## 2 Shigar landscape

This study was undertaken in the SRB which lies exclusively within the Karakoram Range of the Hindu Kush Himalaya (HKH) region of northern Pakistan (Fig. 1a). This landscape is one of the eight subbasins of Upper Indus Basin of the northern mountainous reaches of the Indus River, the main river systems of South Asia. Apart from many other glaciers of Karakoram, glaciers of SRB provide melt water to the Indus River. This landscape covers 7000 km<sup>2</sup> (8.8% of the Karakoram's total land area) and lies between 35.4° and 36.1° N and 74.9° and 76.7° E. This basin, stretching from Ladakh, through Baltistan, southern Xinjiang and up to the north-eastern border of Nagar district is the second largest glacial ice occupied landscape as compared to the eight subbasins of the upper Indus [1]. The southwest boundary of the SRB is surrounded by Shyok River Basin and south-east by Indus basin. It ranges in elevation from 8611 m above sea level (m) at the top of K2 peak to 2775 m at Shigar Bridge, with an average elevation of 4613 m. Distribution of the study area in multiple elevation bands is shown in Fig. 1b. The largest proportion (27.95%) of the total land area of SRB lies between 4510 and 5086 m altitudes followed by 24% between 5086 and 5785 m. At middle elevation, 22.5% lies between 3853 and 4510 m followed by 12.2% between 3000 and 3853 m. The lowest proportion of land area (6%) lies between 5785 and 8572 m.

About 439 glaciers of SRB (~ 7000 km<sup>2</sup>) (Fig. 1a) adhere to mountain sides and therefore do not fit in the primary classification pattern given by RGI Consortium [38]. Only four glaciers of SRB that lie in the Karakoram have largest sizes between 250 and 640 km<sup>2</sup> covering 70.25% or 1534-km<sup>2</sup> glacial area. Portions of these four glaciers that lie inside SRB are extracted from RGI-Version 6.0 [38]. These glaciers include Baltoro glacier (550 km<sup>2</sup> lies within SRB) having more than 25 tributaries, with huge accumulation region that lies at plateaus encircled by high-pitched mountain peaks (e.g. Gasherbrum I and II, Broad Peak, K-2). Biafo glacier (340 km<sup>2</sup> lies within SRB)

**Fig. 1** Map of the study area (Shigar River Basin) within the three Hindu Kush Himalaya (HKH) mountain ranges (Hindu Kush, Himalaya, and Karakoram), the glacier outlines (RGI-V.6) and streams/ rivers (a) extent and hypsometry of the four largest glaciers of Shigar extracted from RGI-V.6 (b)



representing a series of mountain peaks and snow lakes (e.g. 16-km-long Biafo-Hispar) is nourished by more than one accumulation region whose snout joins at low elevation in the valley. Chogo Lungma glacier (230 km<sup>2</sup>) has more or less similar thicknesses from top to bottom, while Panmah glacier (240 km<sup>2</sup>) has smaller children (tributaries) such as Choktoi, Nobande Sobande, Drenmang, Chiring, S. Chiring (Maidan), Shingchukpi and Feriole.

### 3 Materials and methods

#### 3.1 Glacier data

An updated version of glacier dataset (Randolph Glacier Inventory (RGI)-Version 6.0 (released in July 2017 and available on <http://www.glims.org/RGI/randolph60.html>) is used. RGI-Version 6.0 contains outlines of glaciers which are entirely new [38]. DEMs for these larger glaciers of SRB

are extracted from a worldwide compiled, arranged and filtered ASTER global digital elevation model (GDEM2) [12] obtained from <https://earthexplorer.usgs.gov/>. The GeoTIFF format of ASTER GDEM2 used for ELA calculation was available with referenced to the WGS84 geoid and a 1-arc-second 30-m grid of altitude. Therefore, it easily overlapped with glacier outlines of SRB as well. Secondly, for vertical profiles, accuracy of pre-production estimates of digital elevation models was 20 m at 95% confidence and 30 m at 95% for horizontal profiles. We found few pixels with missing data in Shuttle Radar Topography Mission (SRTM). Overall, the accuracy and quality of ASTER GDEM2 digital elevation model used for this study were comparatively consistent for the entire SRB.

### 3.2 Input to AAR and AABR

Hypsometric Integral (HI) toolbox based on the elevation–relief ratio method (Eq. 1) proposed by Pike and Wilson [28] provided by ArcGIS platform of ESRI is used to compute the hypsometric integral (the area lying underneath the standardized hypsometric curve) for SRB. The resulting hypsometric or the experimental cumulative distribution function of altitudes of glaciers of SRB is used as an input to AAR and AABR methods for ELA estimation. The hypsometric curves are made from lowest to highest altitude to represent the ratio of cumulative normalized elevation and cumulative normalized area above the elevation. A higher curve or/and more convex-downward curve indicates slow altitudinal changes in glacier hypsometry.

The relationship is expressed as:

$$HI = (H \text{ mean} - H \text{ minimum}) / (H \text{ maximum} - H \text{ minimum}) \quad (1)$$

where E is the altitude–relief ratio equivalent to the HI (hypsometric integral). H mean is the weighted mean altitude of the basin calculated from the distinguishable elevation contours of the delineated basin. H minimum and H maximum are the lowest and highest altitudes within the glacier.

### 3.3 Equilibrium line altitude (ELA) (AAR, AABR) estimation

ELAs are required to assess hypsometric control of glaciers on their mass balance. An automatic tool developed by Pellitero et al. [30] is used to search and compute the ELA of these glaciers (Baltoro, Biafo, Chogo Lungma and Panmah) of SRB for a given AAR and AABR value by using an iterative procedure which satisfies the mass balance of glacier equation for certain elevation range of the distinctive glacier digital elevation model (DEM). These glaciers

lie transversely in a range of slightly different climatic zones. Initially, we estimated zero net-balance ELAs of each glacier and assumed these four glaciers of SRB are in equilibrium with climatic conditions. AAR and AABR with the lowest standard deviation are as follows: a global ( $1.75 \pm 0.71$ ), high-latitude ( $2.24 \pm 0.85$ ) and Central Asia ( $1.75 \pm 0.56$ ). Similarly, the recommended AARs for cirque and valley glaciers are  $0.6 \pm 0.05$ , debris-covered glaciers between 0.2 and 0.1, etc. Initially, the standard deviation of each AAR and AABR for a group of these four glaciers of SRB was calculated and the AAR (0.6) and AABR (2.24) with the lowest standard deviation were chosen. Iteratively, the elevations corresponding to nine ( $n=9$ ) evenly spaced AAR of between 0.4 and 0.8 (0.4, 0.45, 0.5, 0.55, 0.6, 0.65, 0.7, 0.75, 0.8) and thirty-six ( $n=36$ ) AABR between 0.9 and 4.4 were calculated. The resulting DEMs and the contour intervals for each glacier contour range regions and the ratio ranges for AAR and AABR were stored.

Based on this method, altitudinal area covered by the glacier away from the ELA (either negative or positive) is assumed to have a greater influence to overall mass balance than glacial area that lies nearby to the ELA. This tool follows Cañadas and González-Trueba [10] procedure for the AAR and Osmaston's [25] approach for the AABR. Based on this method, the ratio between the accumulation area and the ablation area was estimated to be constant because they are in steady state ( $HI \sim 0.50$ ) (see Sect. 4.4 and Fig. 5). However, the ratio between these two areas does not take the mass-balance gradient (MBG) controlled by the regional climate and additionally changed by local topo-climatic conditions into account. This tool is based on concepts of [26] for ELA estimation and glacier–climatic reconstruction as it is considered to be more robust than other methods (e.g. the AAR and MGE, median glacier elevation). Glacier hypsometry [25] required by this method along with MBG [6] is given as input.

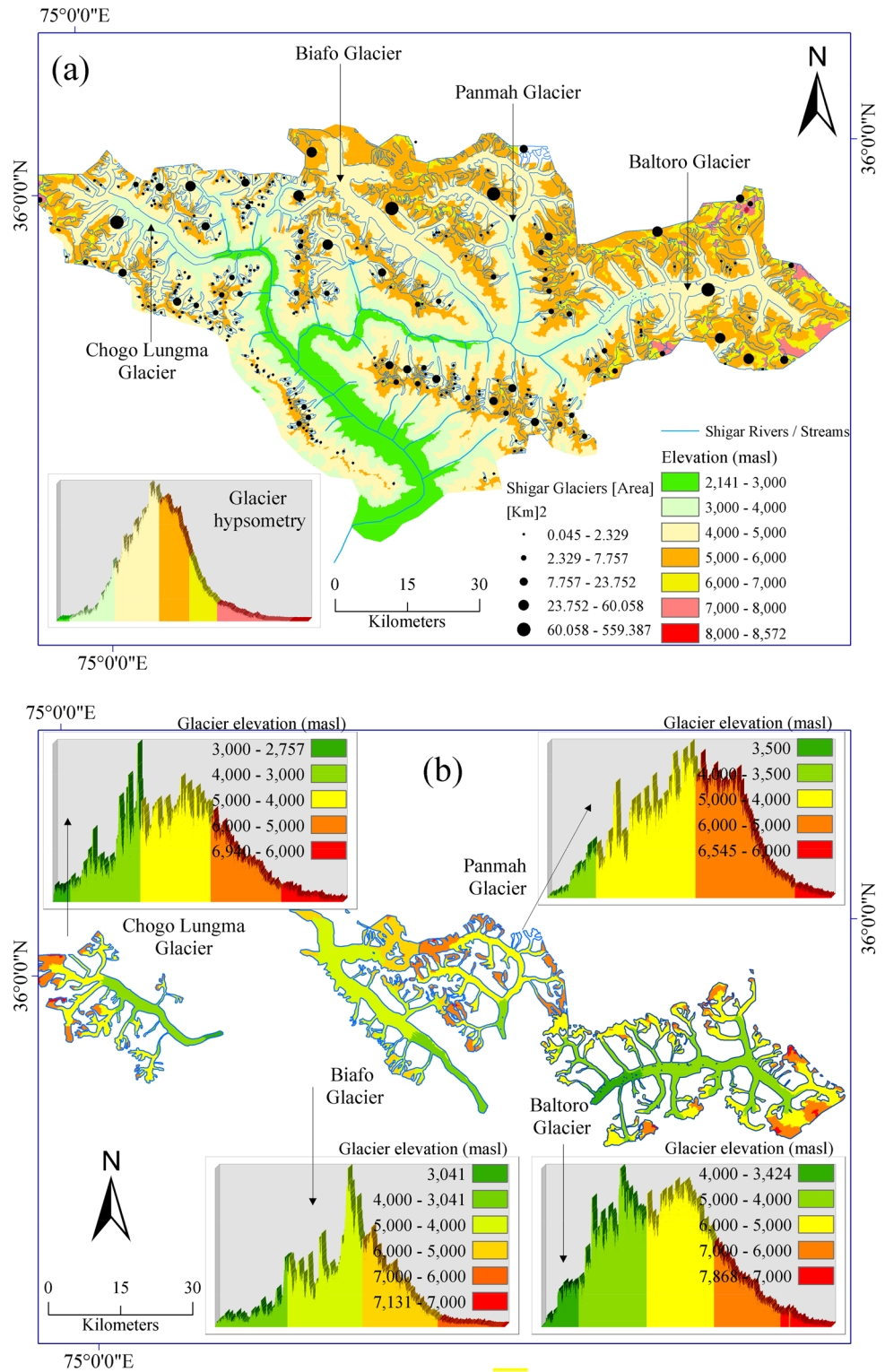
## 4 Results and analysis

### 4.1 Glacier hypsometry

As shown in Fig. 2a, the largest glaciated area (20.63%) of glaciated landscape of SRB lies between 4672 and 5024 m, while the smallest is found in the extreme ends of the altitudinal range ( $\sim 3.26\%$  between 6372 and 8572 m) and ( $\sim 4.12\%$  below 2718–3805 m), mostly debris and clean dust-covered ice. The second largest glaciated area (19.50%) lies between 5024 and 5379 m. Other regions with significant glaciation, 16.63% and 15.50%, lie between 4288 and 4672 m and 5379 and 5793 m, respectively. Mostly, SRB glaciers adhere to mountain sides and therefore do not fit in other primary classification pattern



**Fig. 2** **a** A GIS map representing geographic distribution of SRB glaciers. Glaciers with smallest sizes ( $< 1 \text{ km}^2$ ) are represented with smaller black dots, while largest sizes between 250 and  $640 \text{ km}^2$  with larger black dots. **b** Glacier outlines and their hypsometric curves derived from ASTER GDEM2 data



given by Rau et al. [37]. Half of glaciers or 51.8% of SRB have the smallest sizes ( $< 1 \text{ km}^2$ ), while only four glaciers have the largest sizes between 250 and  $640 \text{ km}^2$  covering 70.25% or  $1534 \text{ km}^2$  glacial area of the SRB. These small glaciers contribute melt water significantly to the Indus

River rise due to their shorter response times as compared to larger glaciers. More details about range of glacier sizes starting from 0.045 to above 250 and their concentration (number of glaciers) on elevations are shown in Fig. 2a. Glacier sizes and distribution of number of glaciers are

presented in the map as well. There are smaller glaciers in the basin than the big ones although it is the four biggest glaciers which occupy more than two-thirds of the glaciated area of Shigar River Basin. Most of the glaciers are located in the north-west, north and north-east of the basin, while only a few small ones are found in the south.

Figure 2b shows the geographic extent (map) and digitally derived hypsometric curves of four main families (types) of SRB glaciers. Chogo Lungma glacier lies in the east, Biafo and Panmah glaciers in the north and Baltoro glacier in the west. Each glacier type along with its tributaries exhibits unique characteristics. (1) Baltoro glacier (~47 km<sup>2</sup> or 7.74% lies in Hunza River Basin and 560 km<sup>2</sup> or 92.26% in SRB) on the border of Xinjiang (China) and Gilgit-Baltistan territory (Pakistan) with huge accumulation region at plateaus encircled by high-pitched mountain peaks (e.g. Gasherbrum I and II, Broad Peak, K-2). The largest glaciated area 18.07% of Baltoro lies between 5321 and 5693 m and smallest (3.89%) between 6622 and 7868 m. (2) Biafo glacier along with its 25 tributaries nourished by more than one accumulation region whose snout join at low elevation in the Shigar valley representing a series of mountain peaks and snow lakes (e.g. 16-km-long Biafo-Hispar). Out of the total 406-km<sup>2</sup> area, 340 km<sup>2</sup> of the 67-km-long Biafo glacier lies in SRB. The largest glaciated area (24.71%) of this glacier lies at 4240–4623 m elevation, while the smallest area lies in the extreme ends of the altitudinal range ~1.71% between 5956 and 7131 m and ~4.7% between 3041 and 3753 m. (3) Chogo Lungma glacier (45.3 km long covering 230 km<sup>2</sup> of SRB) has irregular thicknesses from top to bottom. The largest glaciated area (35.13%) of this glacier lies between 4271 and 4969 m and the smallest portion (3.16%) between 5870 and 6940 m. (4) About 44-km-long Panmah family of glaciers occupy 274 km<sup>2</sup> area by its smaller children (tributaries) like Choktoi, Nobande Sobande, Drenmang, Chiring, S. Chiring (Maidan), Shingchukpi and Feriole. The largest glaciated area (34.59%) of Panmah glacier lies between 4877 and 5370 m and the smallest (4.75%) between 5678 and 6503 m.

## 4.2 Vertical and horizontal climatic regimes

Precipitation plays a vital role in the snow and glacial accumulation and temperature in ablation, respectively. Therefore, it is imperative to create a relationship between climatic conditions and glacier accumulation/ablation. Two graphs (histograms) representing hypsometric distribution of glaciated (Fig. 3a) and non-glaciated land area (Fig. 3b) are presented. The x-axis and y-axis of these graphs (histograms) represent the vertical climatic regimes (e.g. net melting, ablation melt/freeze, high-altitude melt, 0 °C isotherm, net freezing/accumulation, avalanche

nourishment and perennial snow and ice) and horizontal climatic regimes (e.g. net ablation, mixed and net accumulation), respectively. Regional (Karakoram) ELAs estimated by Wake [40] and Mukhopadhyay et al. [21] for two different years are overlaid over these histograms of these two landscapes. The largest glaciated area (20.60%) between 4000 and 4500 m lies in the vertical regime of direct snow-accumulation zone and in the horizontal regime of net-accumulation zone (low velocity, net freezing and no sliding). At this elevation range, the mean annual temperature and precipitation remain –10 to –13 °C and 1900 to 2000 mm, respectively. Secondly, the second largest glaciated area (16.60%) between 3500 and 4000 m lies in the vertical regime of ice fall and clean/dusty ice region and mostly in the horizontal regime of mixed zone (high glacier velocity and net accumulation zone with low velocity). At this elevation, the mean annual temperature and precipitation are between –5 and –10 °C and 1900 and 2100 mm, respectively. The smallest area of glaciated landscape (3.26%) and (4.12%) lies in the extreme ends of the highest (between 5500 and 8572 m) and lowest (between 2141 and 3000 m) elevation range, respectively. Glaciated area at highest elevation corresponds to snow and perennial ice and snow debris-covered ice of vertical regime and at lowest elevations corresponds to net melting of vertical regime and net ablation of horizontal regime, where mean annual temperature remains above +10 °C.

## 4.3 Zero-net balance ELA for glacier equilibrium

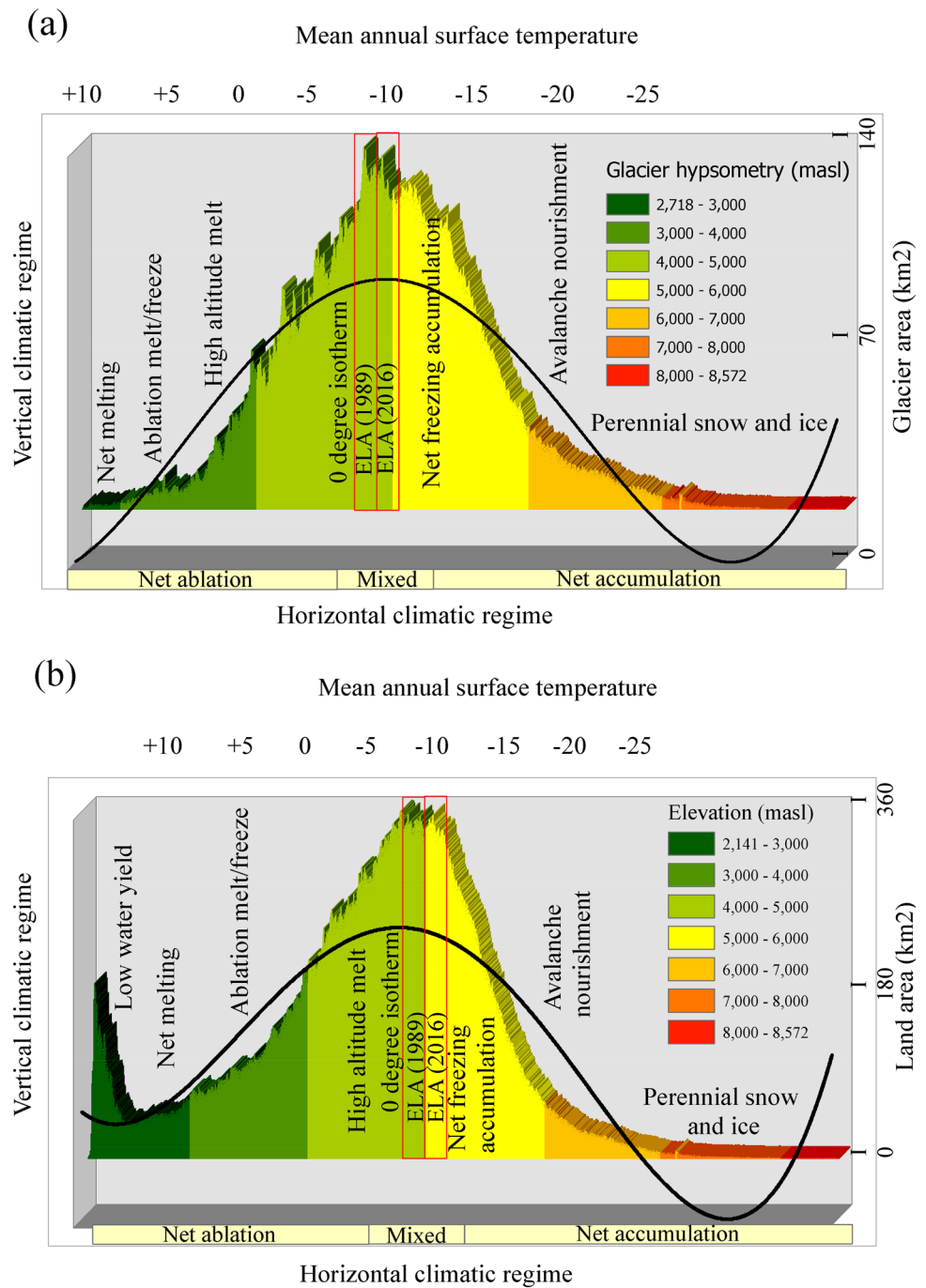
We estimated zero net-balance ELAs and assumed these four glaciers of SRB are in equilibrium with climatic conditions. Figure 4 shows maps of reconstructed glacial-ice areas and contours corresponding to estimate zero net-balance ELAs of four largest SRB glaciers. Based on recommended values of (AAR=0.6) for mountain glaciers, a linear regression examination recommends that the zero net-balance ELA for zero-specific mass balance is ~5545 m for Baltoro glacier. Similarly, Biafo glacier lies in the northern region of SRB; the ELA for zero-specific mass balance is 4987 m as compared to 5056 m for Panmah glacier and 4822 m for Chogo Lungma glacier.

## 4.4 Accumulation-area above and ablation-area below ELA

Ratios between accumulation area, ablation area and the total glacial area of these glaciers are estimated for lowest AAR (0.4) and AABR (0.9), highest AAR (0.8) and AABR (4.4) and recommended AAR value (0.6) and AABR (2.24), respectively (Fig. 5).

Firstly, majority (41.68%) of the Baltoro glacier lies at transitional altitudes, especially in the 4000–6000-m

**Fig. 3** Histograms representing hypsometric distribution of the glaciated and non-landscapes of SRB along with vertical and horizontal climatic regimes and regional ELAs obtained from literature values for two years (1989 and 2016). **a** Histogram (glacial ice area occupied by glacier outlines proportional to the frequency of glaciated elevations), positions of Karakoram ELAs and mean annual temperature (°C). **b** Histogram (land area occupied by non-glaciated land area proportional to the frequency of elevations), positions of Karakoram ELAs and mean annual temperature (°C)



region where the hypsometric curve is much flatter. The accumulation area (35%) is limited to the vertical (steeper) region of the curve (below 5545 m) and 65% ablation area for AAR (0.6) as compared to (below 5279 m) covering 42% accumulation area and 58% ablation area for AABR (2.24) to the total glacial area. An increase in the AAR from lowest (0.4) to highest (0.8) reduces 900-m ELA of Baltoro glacier from 5769 to 4869, a ~40% reduction in accumulation area. Similarly, an increase in the AABR from lowest (0.9) to highest (4.4) reduces 490-m ELA of Baltoro glacier from

5579 to 5089 m, a ~30% reduction in accumulation area. Secondly, majority (43.32% glacial area) of the Biafo glacier lies at middle altitudes between 4500 and 5700 m where the hypsometric curve is sloping. The ELA accumulation area is limited to the vertical (steeper) region of the curve (below 4987 m) covering 43% accumulation area and 67% ablation area for AAR (0.6) as compared to (below 4766 m) covering 58% accumulation area and 42% ablation area for AABR (2.24) to the total glacial area. An increase in the AAR from lowest (0.4) to highest (0.8) reduces 650-m ELA

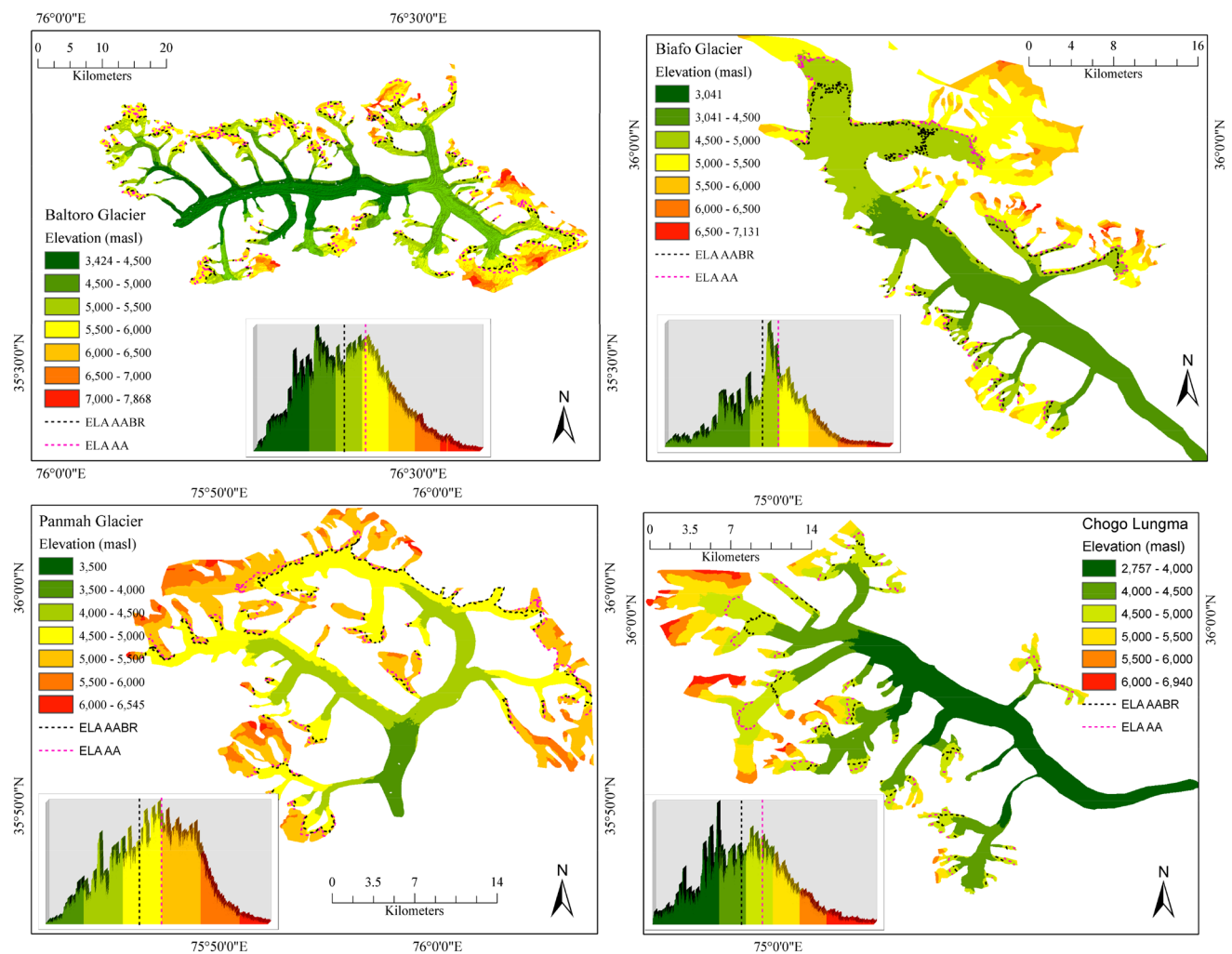


**Fig. 4** Maps of reconstructed glacier area and contours corresponding to respective ELAs (AAR of 0.6 and AABR of 2.24) of four largest glaciers of SRB of the Karakoram. The slightly different ELA

estimates between the AAR and AABR methods can be attributed to a few methodical differences

of Biafo glacier from 5216 to 4566, a ~50% reduction in accumulation area. Similarly, an increase in the AABR from lowest (0.9) to highest (4.4) reduces 600-m ELA of Biafo glacier from 5216 to 4616 m, a ~50% reduction in accumulation area. Thirdly, unlike Baltoro and Biafo, the majority of the Chogo Lungma glacier lies at transitional altitudes (between 3500 and 5500 m) where the hypsometric curve represents positive slope (increasing from lower to higher elevation), and 81% of the area of the glacier lies between this elevation range. The ELA accumulation area is limited to the vertical (steeper) region of the curve (below 4682 m) covering 61% accumulation area and 39% ablation for AAR (0.6) as compared to (below 4582 m) covering 50% accumulation area and 50% ablation for AABR (2.24) to the total glacial area. An increase in the AAR from lowest (0.4) to highest (0.8) reduces 850-m ELA of Chogo Lungma glacier from 5082 to 4232 m, a ~38% reduction in

accumulation area. Similarly, an increase in the AABR from lowest (0.9) to highest (4.4) reduces 450-m ELA of Chogo Lungma from 4832 to 4382 m, a ~30% reduction in accumulation area. Lastly, the majority of the Panmah glacier lies at high altitude, especially between 4700 and 5500 m elevation range where the hypsometric curve is little bit sloping; 61% of the area of the glacier lies between this elevation range. The ELA accumulation area is limited to the vertical (steeper) region of the curve (below 4955 m) covering 52% accumulation area and 48% ablation area to the total glacial area for both AAR (0.6) and AABR (2.24) below 4895 m. An increase in the AAR from lowest (0.4) to highest (0.8) reduces 600-m ELA of Panmah glacier from 5235 to 4635 m, a ~40% reduction in accumulation area. Similarly, an increase in the AABR from lowest (0.9) to highest (4.4) reduces 320-m ELA of Panmah from 5075 to 4755 m, a ~26% reduction in accumulation area.



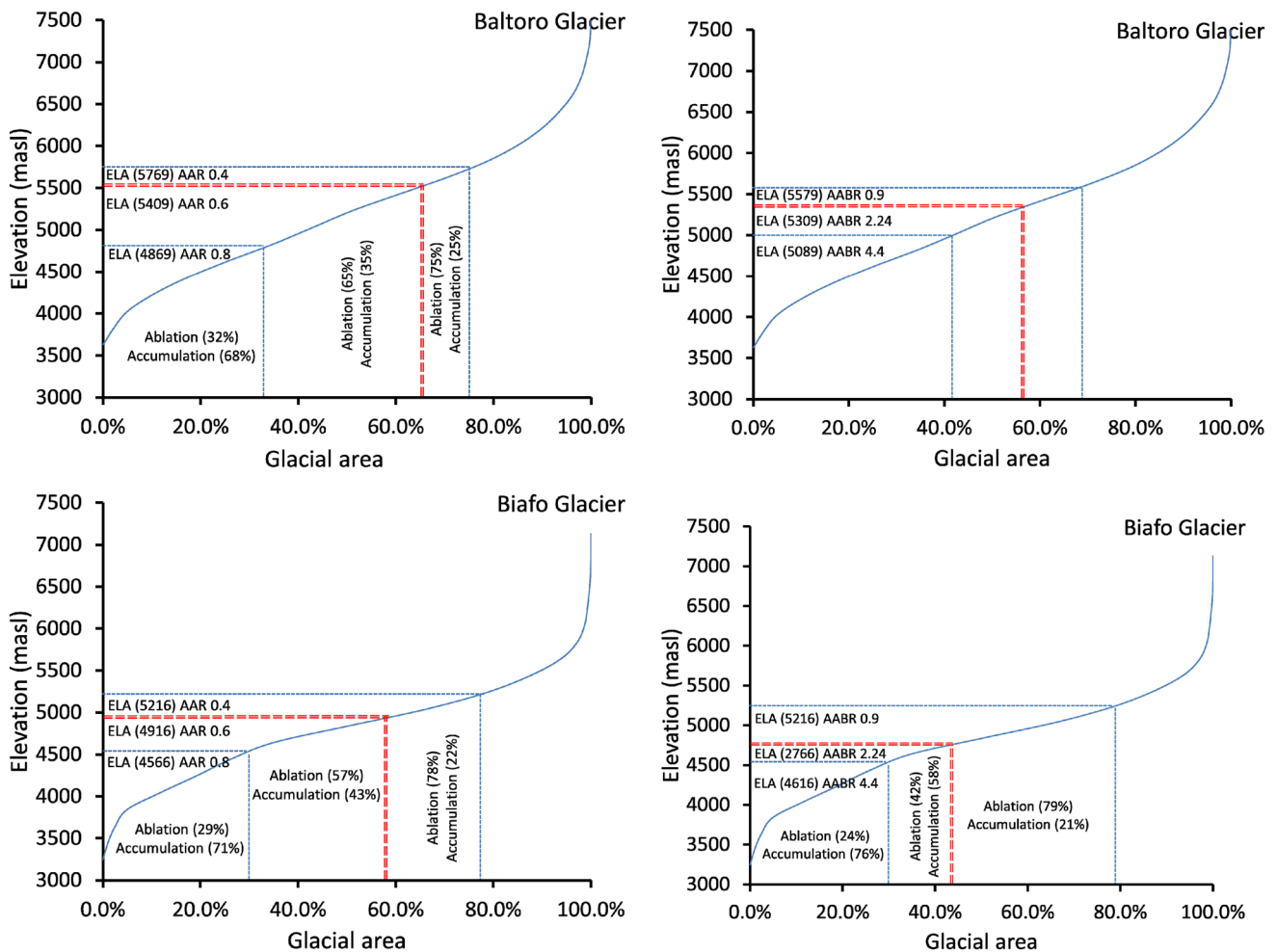


**Fig. 5** The elevation range (in masl) of four glaciers (Baltoro, Biafo, Chogo Lungma and Panmah) plotted against their cumulative percentage area of the surfaces for three constants values of AAR (0.4, 0.6 and 0.8) with an interval of 0.2 and AABR (0.9, 2.24 and 4.4) with

an interval of 1.40. The cumulative percentage area of the glacier surfaces within the contours corresponding to the ELA AAR (0.6) and ELA AABR (2.24) is highlighted

### 4.5 ELA sensitivity to AAR and AABR

By providing constant AAR (rather than constant glacier area), this approach accustomed glacier geometries to future ELA surges. For example, for constant AAR (0.4–0.45), a 90-m ELA decrease from 5769 to 5679 m of Baltoro glacier adjusted its geometries by reducing ~5% area. The highest decrease of 140-m ELA of the same glacier is reported for constant AAR (0.7–0.75), revealing a significant loss of 8% geometries. Variations in the adjustment of glacier geometries as a result of changing ratios of ELA AAR (Fig. 6a) and ELA AABR (Fig. 6b) for largest four glaciers of SRB are compared and presented. Lists of constant AAR (0.4–0.8) ratios are presented in Table 1 and AABR (1.0–4.4) in Table 2. Projected geometry (area) losses for all these glaciers are highly variable, with top-heavy glaciers (Biafo and Baltoro) projected to experience the utmost major losses at elevation

(5000–5500 m) in glacier-ice area. Lowest glacier area losses are reported at lowest elevations for AAR. Our results suggest that a 100-m ELA (Fig. 6a) decrease will increase the number of SRB glaciers by 10%, while increasing glacier area by 15% and glacier volume by 12%. A more aggressive ELA decrease of 200 m (Fig. 6b) yields increment of 40%, 30% and 22%, respectively (Fig. 6b). Losses are principally determined by variations in the smaller glaciers (e.g. Panmah and Chogo Lungma) that have slim altitude ranges (Fig. 2b). Additionally, potential for significant loss is high in middle elevation ranges.

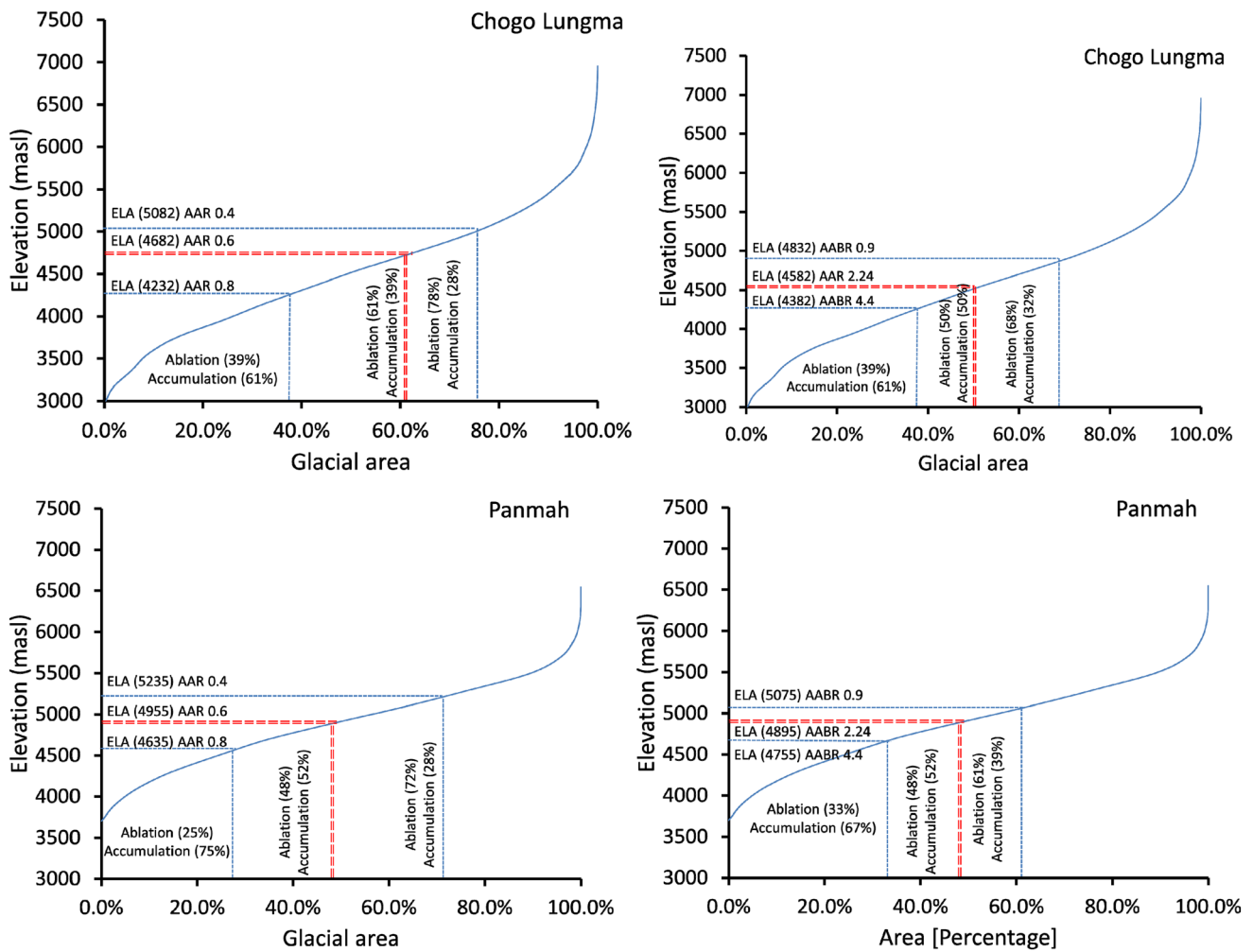


Fig. 5 (continued)

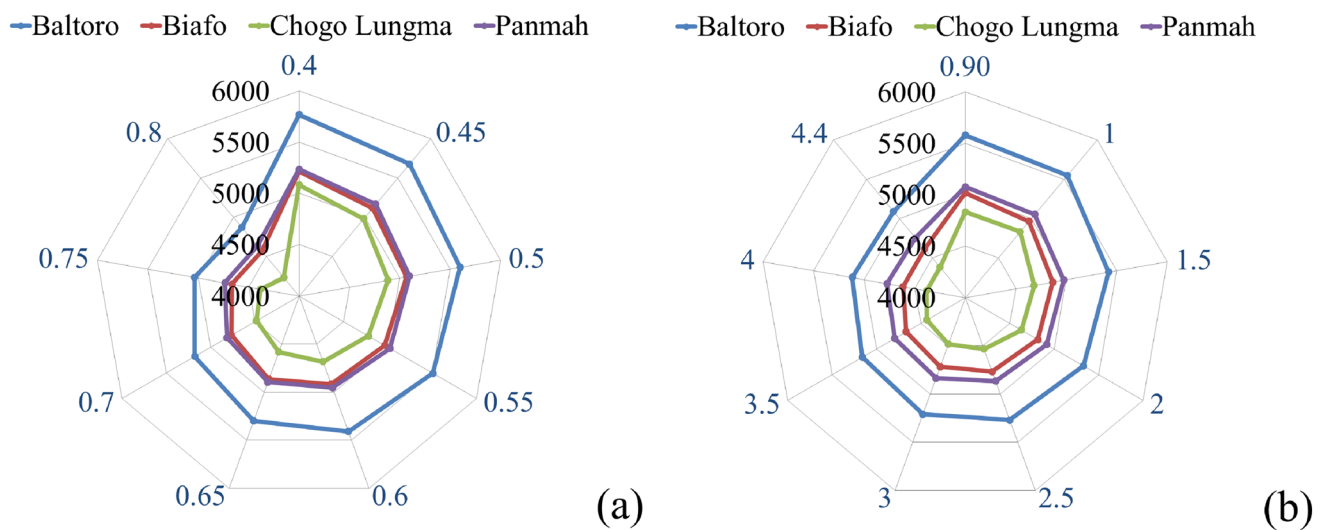


Fig. 6 Adjustment of glacier geometries to future ELA variations for constant AAR (between 0.4 and 0.8) with 0.05 interval (a) and ABR (between 0.9 and 4.4) with 0.5 interval (b)

**Table 1** Decrease in equilibrium line altitude (ELA) of four glaciers (Baltoro, Biafo, Chogo Lungma and Panmah) for constant AAR (0.40–0.80) with 0.05 interval

	Values	Baltoro GL (ELA in meters)	Biafo GL (ELA in meters)	Chogo Lungma GL (ELA in meters)	Panmah GL (ELA in meters)
AAR <sub>1</sub>	0.40	5769	5216	5082	5235
AAR <sub>2</sub>	0.45	5679	5116	4982	5165
AAR <sub>3</sub>	0.50	5599	5066	4882	5095
AAR <sub>4</sub>	0.55	5509	4966	4782	5025
AAR <sub>5</sub>	0.60	5409	4916	4682	4955
AAR <sub>6</sub>	0.65	5299	4866	4582	4895
AAR <sub>7</sub>	0.70	5179	4766	4482	4815
AAR <sub>8</sub>	0.75	5039	4666	4382	4735
AAR <sub>9</sub>	0.80	4869	4566	4232	4635

## 5 Discussion

Firstly, for zero mass balance, AAR values of 0.58 for the North Cascade glaciers [23] and 0.7 for the Alpine glaciers [32] were suggested, respectively. We used the AAR value of 0.6 and AABR value of 2.24 for their respective zero mass balance for glaciers of SRB due to their high-altitude settings. A decreasing trend in ELA for a range of initial AAR values (0.4–0.8) is observed for these glaciers unlike initial AABRs values (0.90–4.4). The difference in the ELA between AAR and AABR methods indicates that the AABR method is appropriate to estimate ELA of clean-ice covered and snow-fed glaciers (Pellitero et al., 2013), but we tested for debris-covered glaciers; therefore, the AABR ELA needs to be verified through field data. Glacier hypsometry provides a first-order estimator of glacier mass-balance sensitivity to the variation in ELAs [30]. However, similar to McGrath et al., [22], regional climatic change (e.g. increase in temperature) in the high mountain Karakoram region may fluctuate the ELAs of individual glaciers to a critical point, whereby a small additional increase in the ELA may result in a substantial loss of accumulation area, with a prominent consequence for the inclusive behaviour of the Karakoram glaciers. Based on these results, we assume that there is a relationship between the ratio of accumulation area of Shigar glaciers and the scale of variation in ELA. About 70% of the glaciers of SRB have altitude ranges below ~6000 m and 48% below 4200 m. An increase in ELA is likely and will affectively decrease the accumulation area as half of SRB glaciers or 51.8% have the smallest sizes (< 1 km<sup>2</sup>). Glacier altitude range of each glacier is correlated with its glacier-ice area, suggesting that losses will be most noticeable for more than 220 smaller glaciers (< 1 km<sup>2</sup>), while the larger studied glaciers (e.g. Baltoro, Biafo, Panmah and Chogo Lungma) are progressively less sensitive. This sensitivity does not exhibit a simple relationship, reflecting the abundance and comparatively homogeneous dispersal of small glaciers throughout the entire

basin. However, the overall quality of the ELAs is highly dependent on the reconstructed three-dimensional (3D) glacier surfaces [27].

A number of limitations are still present in this study: field-based mass-balance data are not available for Karakoram glaciers to cross-check these results. Therefore, these methods may produce less accurate results. However, shifting of the ELA due to the influence of variation in the magnitude and seasonality of snowfall cannot be ignored. This paper does not determine response time of glacier volume of SRB. However, variations in the positions of two ELAs (calculated based on AAR and AABR) for each glacier type determine the differences in accumulation ratios produced by two methods. Secondly, the study area should not be considered as a representative of the glaciated and non-glaciated landscapes of the entire Karakoram Range.

## 6 Conclusion

AAR- and AABR-based estimation of ELAs by using ArcGIS toolbox was efficient, less time-consuming and easier to use. However, the overall quality of the ELAs is highly dependent on the reconstructed three-dimensional glacier surfaces. The method we used has the capability to reconstruct two-dimensional glacier surfaces followed by three-dimensional glacier reconstructions for three-dimensional area calculation above and below the ELAs. However, the interpretations of glacier surfaces of SRB by using our own perspective may be slightly different from other researchers' point of view. A slight difference in the ELA between AAR and AABR methods (Fig. 4) indicates that the AABR method is appropriate to estimate ELA of clean-ice covered and snow-fed glaciers. But we tested for debris-covered glaciers; therefore, AABR estimates need to be supported by field data. We used the AAR value of 0.6 and AABR value of 2.24 for their respective zero mass balance for SRB glaciers due to their high-altitude settings.

**Table 2** Decrease in equilibrium line altitude (ELA) of four glaciers (Baltoro, Biafo, Chogo Lungma and Panmah) for constant AABR (0.90–4.4) with 0.01 interval

AABR	Baltoro GL (ELA in meters)	Biafo GL (ELA in meters)	Chogo Lungma GL (ELA in meters)	Panmah GL (ELA in meters)
0.90	5579	5016	4832	5075
1.00	5549	4966	4832	5055
1.10	5519	4966	4782	5035
1.20	5489	4966	4782	5015
1.30	5469	4916	4732	5005
1.40	5439	4916	4732	4985
1.50	5419	4866	4682	4975
1.60	5399	4866	4682	4965
1.70	5379	4866	4682	4945
1.80	5369	4816	4632	4935
1.90	5349	4816	4632	4925
2.00	5329	4816	4632	4915
2.10	5319	4816	4582	4905
2.20	5309	4766	4582	4895
2.30	5289	4766	4582	4885
2.40	5279	4766	4582	4875
2.50	5269	4766	4532	4865
2.60	5249	4766	4532	4865
2.70	5239	4716	4532	4855
2.80	5229	4716	4532	4845
2.90	5219	4716	4482	4835
3.00	5209	4716	4482	4835
3.10	5199	4716	4482	4825
3.20	5189	4666	4482	4815
3.30	5179	4666	4482	4815
3.40	5169	4666	4432	4805
3.50	5159	4666	4432	4795
3.60	5149	4666	4432	4795
3.70	5139	4666	4432	4785
3.80	5139	4666	4432	4785
3.90	5129	4616	4432	4775
4.00	5119	4616	4382	4775
4.10	5109	4616	4382	4765
4.20	5109	4616	4382	4765
4.30	5099	4616	4382	4755
4.40	5089	4616	4382	4755

In this study, we assumed that altitudinal area covered by the glacier away from the ELA (either negative or positive) has a greater influence to overall mass balance than glacial area close to the ELA. As compared to AAR, AABR still gives a sign of the mass balance although under no circumstances this is an outright estimation. It simply indicates that there is nonlinearity in the accumulation (increase/decrease) and/or that the gradient is overvalued. In this study, AABR is used as a sign of the means by which these

four glaciers diverge from the assumed linearity (zero mass-balance curves). By recommending constant values for AAR and AABR (rather than glacier area) for mountain glaciers, the dynamic response method modifies glacier geometries to future ELA decreases. These estimates are not yet supported by field data. An extensive series of field data is required for better understanding of the relationship between these parameters.

**Acknowledgement** Firstly, the authors would like to thank Dr. Humaira Khan and Dr. Bahadar Nawab Khattak for their encouragement and continuous support. Secondly, the authors thank ASTER for enabling us to download DEMs. Special thanks go to anonymous reviewers for their comments which helped to improve this work.

**Conflict of interest** On behalf of all authors, the corresponding author states that there is no conflict of interest.

**Open Access** This article is licensed under a Creative Commons Attribution 4.0 International License, which permits use, sharing, adaptation, distribution and reproduction in any medium or format, as long as you give appropriate credit to the original author(s) and the source, provide a link to the Creative Commons licence, and indicate if changes were made. The images or other third party material in this article are included in the article's Creative Commons licence, unless indicated otherwise in a credit line to the material. If material is not included in the article's Creative Commons licence and your intended use is not permitted by statutory regulation or exceeds the permitted use, you will need to obtain permission directly from the copyright holder. To view a copy of this licence, visit <http://creativecommons.org/licenses/by/4.0/>.

## References

1. Bajracharya SR, Maharjan SB, Shrestha F (2019) Glaciers in the Indus basin. Int Centre Integr Mountain Dev, Kathmandu, Nepal. <https://doi.org/10.1016/B978-0-12-812782-7.00006-0>
2. Bajracharya SR, Shrestha B (2011) The status of glaciers in the Hindu Kush-Himalayan region. International Centre for Integrated Mountain Development, Kathmandu
3. Bakke J, Nesje A (2011) Equilibrium-line altitude (ELA). In: Singh V, Singh P, Haritashya U (eds) Encyclopedia of snow, ice and glaciers. Springer, Netherlands, pp 268–277
4. Baig SU, Khan H, Din A (2018) Spatio-temporal analysis of glacial ice area distribution of Hunza River Basin, Karakoram region of Pakistan. Hydrol Process 32:1491–1501. <https://doi.org/10.1002/hyp.11508>
5. Benn DI, Ballantyne CK (2005) Palaeoclimatic reconstruction from Loch Lomond Readvance glaciers in the West Drumochter Hills Scotland. Quat Sci Rev 20:577–592
6. Benn DI, Lehmkuhl F (2000) Mass balance and equilibrium line altitudes of glaciers in high mountain environments. Quatern Int 65(66):15–29. [https://doi.org/10.1016/S1040-6182\(99\)00034-8](https://doi.org/10.1016/S1040-6182(99)00034-8)
7. Braithwaite RJ, Raper SCB (2009) Estimating equilibrium-line altitude (ELA) from glacier inventory data. Ann Glaciol 50(53):127–132. <https://doi.org/10.3189/172756410790595930>
8. Bhambri R, Hewitt K, Kawishwar P, Pratap B (2017) Surge-type and surge-modified glaciers in the Karakoram. Sci Rep 7(1):1–14. <https://doi.org/10.1038/s41598-017-15473-8>



9. Bhambri R, Hewitt K, Kawishwar P, Kumar A, Verma A, Tiwari S, Misra A (2019) Ice-dams, outburst floods, and movement heterogeneity of glaciers, Karakoram. *Global Planet Change* 180:100–116. <https://doi.org/10.1016/j.gloplacha.2019.05.004>
10. Cañadas ES, González Trueba J (2013) The AAR method (accumulation area ratio) for palaeo-ELAs reconstruction: methodological analysis and application in the Valdecebollas Massif (Cantabrian Mountains). *Cuadernos de Investigación Geográfica* 30:7–34
11. Dyurgerov M, Meier MF, Bahr DB (2009) A new index of glacier area change: a tool for glacier monitoring. *J Glaciol* 55(192):710–716. <https://doi.org/10.3189/002214309789471030>
12. Fujisada H, Urai M, Iwasaki A (2012) Technical methodology for ASTER global DEM. *IEEE Geosci Remote Sens Soc* 50:3725–3736. <https://doi.org/10.1109/TGRS.2012.2187300>
13. Hewitt K (2011) Glacier change, concentration, and elevation effects in the Karakoram Himalaya, Upper Indus Basin. *Mountain Res Dev* 31:188–200. <https://doi.org/10.1659/MRD-JOURN-AL-D-11-00020.1>
14. Hewitt K, Wake CP, Young GJ, David C (1989) Hydrological investigations at Biafo glacier, Karakoram Himalaya—An important source of water for the Indus River. *Ann Glaciol* 13:103–108
15. Hughes PD (2009) Twenty-first century glaciers and climate in the Prokletije Mountains, Albania. *Arct Antarct Alp Res* 41(4):455–459. <https://doi.org/10.1657/1938-4246-41.4.455>
16. IPCC (2014) Climate change 2014: synthesis report. In: Core Writing Team, Pachauri RK, Meyer LA (eds) Contribution of working Groups I, II and III to the fifth assessment report of the intergovernmental panel on climate change. IPCC, Geneva
17. Lukas S (2007) Early-Holocene glacier fluctuations in Krundalen, south central Norway: palaeo-glacier dynamics and palaeoclimate. *Holocene* 17:585–598
18. Lachniet MS, Seltzer G (2004) Late quaternary glaciation of Costa Rica and Guatemala Central America. *Dev Quat Sci* 2(1):135–138. [https://doi.org/10.1016/S1571-0866\(04\)80118-0](https://doi.org/10.1016/S1571-0866(04)80118-0)
19. Majeed U, Rashid I (2020) Evaluating glacier surges in Karakoram region using earth observation data. *Data Brief* 351:105394. <https://doi.org/10.1016/j.dib.2020.105394>
20. Mölg N, Bolch T, Rastner P, Strozzi T, Paul F (2018) A consistent glacier inventory for Karakoram and Pamir derived from Landsat data: distribution of debris cover and mapping challenges. *Earth Syst Sci Data* 10:1807–1827. <https://doi.org/10.5194/essd-10-1807-2018>
21. Mukhopadhyay B, Khan A (2017) Altitudinal variations of temperature, equilibrium line altitude, and accumulation-area ratio in Upper Indus Basin. *Hydrol Res* 48(1):214–230. <https://doi.org/10.2166/nh.2016.144>
22. McGrath D, Sass L, O’Neel S, Arendt A, Kienholz C (2017) Hypsometric control on glacier mass balance sensitivity in Alaska and northwest Canada. *Earth’s Future* 5(3):324–336. <https://doi.org/10.1002/2016EF000479>
23. Meier MF, Post A (1962) Recent variations in mass net budgets of glaciers in western North America international association of scientific hydrology. *Symp Oberurgul, Publ Number* 58(1962):63–77
24. Mayer C, Lambrecht A, Belò M, Smiraglia C (2006) Glaciological characteristics of the ablation zone of Baltoro glacier Karakoram, Pakistan. *Ann Glaciol* 43:123–131. <https://doi.org/10.3189/172756406781812087>
25. Osmaston HA (2005) Estimates of glacier equilibrium line altitudes by the Area×Altitude, the Area×Altitude Balance Ratio and the Area×Altitude Balance Index methods and their validation. *Quat Int* 138(139):22–31. <https://doi.org/10.1016/j.quaint.2005.02.004>
26. Osmaston H (1965) The past and present climate and vegetation of Ruwenzori and its neighbourhood. D.Phil thesis, University of Oxford, Oxford
27. Pearce D, Ely J, Barr LD, Boston CM (2017) Glacier reconstruction, ISSN 2047–0371. University of Aberdeen, School of Geosciences
28. Pike RJ, Wilson SE (1971) Elevation–relief ratio, hypsometric integral and geomorphic area–altitude analysis. *Geol Soc Am Bull* 82:1079–1084
29. Pellitero R (2013) Evolución fincuaternaria del glaciario en el macizo de Fuentes Carrionas (Cordillera Cantábrica), propuesta cronológica y paleoambiental. *Cuaternario y Geomorfología* 27(1–2):71–90
30. Pellitero R, Rea BR, Spagnolo M, Bakke J, Hughes P, Ivy-Ochs S, Lukas S, Ribolini A (2015) A GIS tool for automatic calculation of glacier equilibrium-line altitudes. *Comput Geosci* 82:55–62. <https://doi.org/10.1016/j.cageo.2015.05.005>
31. Porter S (2001) Snowline depression in the tropics during the last Glaciation. *Quatern Sci Rev* 20:1067–1091
32. Paterson, W.S.B (1981) *The Physics of Glaciers*, Pergamon Press, ISBN: 9780080240060 <https://books.google.com.pk/books?id=S3J>
33. Rashid I, Abdullah T, Glasser NF, Naz H, Romshoo SA (2018) Surge of Hispar Glacier, Pakistan, between 2013 and 2017 detected from remote sensing observations. *Geomorphology* 303:410–416. <https://doi.org/10.1016/j.geomorph.2017.12.018>
34. Rashid I, Majeed U, Jan A, Glasser NF (2020) The January 2018 to September 2019 surge of Shisper Glacier, Pakistan, detected from remote sensing observations. *Geomorphology* 351:106957. <https://doi.org/10.1016/j.geomorph.2019.106957>
35. Racoviteanu AE, Rittger K, Armstrong R (2019) An automated approach for estimating snowline altitudes in the Karakoram and eastern Himalaya from remote sensing. *Front Earth Sci* 7:220. <https://doi.org/10.3389/feart.2019.00220>
36. Raper SCB, Braithwaite RJ (2009) Glacier volume response time and its links to climate and topography based on a conceptual model of glacier hypsometry. *The Cryosphere* 3:183–194. <https://doi.org/10.5194/tc-3-183-2009>
37. Rau F, Mauz F, Vogt S, Singh SJ, Khalsa, Raup B (2005, version-1.0) Glacier classification guidance for the GLIMS glacier inventory, Institute of Physical Geographaphy, Frieburg (Germany), and National Snow and Ice Data Center, Boulder, CO (USA). (<http://www.glims.org> Accessed on 2019–05–18)
38. RGI Consortium (2017) Randolph glacier inventory (RGI)—a dataset of global glacier outlines: Version 6.0. Technical Report, Global Land Ice Measurements from Space, Boulder, Colorado, USA. Digital Media. <https://doi.org/10.7265/N5-RGI-60>
39. Stansell ND, Pratigya PJ, Abbott MB (2007) Last glacial maximum equilibrium-line altitude and paleo-temperature reconstructions for the Cordillera de Mérida Venezuelan Andes. *Quat Res* 67(2007):115–127. <https://doi.org/10.1016/j.yqres.2006.07.005>
40. Wake CP (1989) Glaciochemical investigations as a tool for determining the spatial and seasonal variation of snow accumulation in the central Karakoram, northern Pakistan. *Ann Glaciol* 13:279–284
41. Zasadni J, Świąder A, Kłapyta P (2018) A novel (raster input/output) method of equilibrium line altitude (AAR, AABR) estimation and glacier hypsometry analysis. *Geophys Res Abstracts* 20:18556

**Publisher’s Note** Springer Nature remains neutral with regard to jurisdictional claims in published maps and institutional affiliations.